Journal of Macromolecular Science, Part A
Publication details, including instructions for authors and subscription information:
http://www.informaworld.com/smpp/title~content=t713597274

Nonequilibrium Flow and the Kinetics of Chemical Reactions in the Char Zone

Gary C. April[a]; Ralph W. Pike[a]; Eduardo G. Del Valle[a]
[a] Department of Chemical Engineering, Louisiana State University, Baton Rouge, Louisiana

To cite this Article April, Gary C. , Pike, Ralph W. and Valle, Eduardo G. Del(1969) 'Nonequilibrium Flow and the Kinetics of Chemical Reactions in the Char Zone', Journal of Macromolecular Science, Part A, 3: 4, 685 — 704
To link to this Article: DOI: 10.1080/10601326908053836
URL: http://dx.doi.org/10.1080/10601326908053836

J. MACROMOL. SCI.–CHEM., A3(4), pp. 685-704, July, 1969

Nonequilibrium Flow and the Kinetics of Chemical Reactions in the Char Zone

GARY C. APRIL, RALPH W. PIKE, and EDUARDO G. DEL VALLE

Department of Chemical Engineering
Louisiana State University
Baton Rouge, Louisiana

SUMMARY

In the temperature range of 500-2500°F, nonequilibrium flow analysis predicted only a small change in pyrolysis gas composition as the gases flow through the char zone. Essentially all of the reactions took place in the temperature range of 2000-2500°F. Comparing nonequilibrium flow with the two limiting cases, the energy absorbed in the char zone for frozen flow was two-thirds that of nonequilibrium flow, and equilibrium flow was about four times that of nonequilibrium flow at the 2500°F level.

Experimental results were obtained simulating the char zone during ablation in the temperature range of 700-1650°F using the char zone thermal environment simulator. The data showed that the flow was essentially frozen, and this was accurately predicted by the nonequilibrium flow analysis. The limiting case of equilibrium flow incorrectly predicted significant changes in the pyrolysis gas composition over the temperature range investigated.

INTRODUCTION

The primary objective of this research program is to determine accurately the energy absorbed in the char zone of a charring ablator and how

this is affected by the chemical reactions that occur within the char. At present, there are two methods available to describe the limits on the heat transfer in the char zone. These are referred to as the frozen flow and equilibrium flow cases.

The minimum amount of energy that can be absorbed in the char zone can be computed by considering the flow to be frozen. This refers to the situation where the pyrolysis gases flowing through the char do not undergo any chemical reactions (the composition is constant). The amount of energy absorbed is given by the change in sensible heat of the gases.

The maximum amount of energy that can be absorbed in the char zone is obtained by considering the chemical species in the flow field to be in thermodynamic equilibrium. This refers to the situation where the degradation products undergo reaction at an infinitely fast rate, and the amount of energy absorbed is computed by considering the species to be in thermodynamic equilibrium. This gives the maximum energy absorbed since the reactions are nearly all endothermic.

The limits on the energy transfer established by these two cases have been reported previously [1, 2]. It was found that the amount of energy that could be absorbed was almost an order of magnitude greater for equilibrium flow than for frozen flow for the same front- and back-surface temperatures on the char. Due to the high mass flux of gases from the plastic decomposition, the actual amount of energy that is absorbed lies somewhere between these two limiting cases and is determined by the rates of chemical reaction among the species present.

In this paper the necessary equations are presented for computing the energy absorbed in the char zone. These equations are solved for non-equilibrium flow in the char and for the two limiting cases of frozen and equilibrium flow. Comparisons are made between the computed results and experimental data obtained with the char zone thermal environment simulator. Details are given for the generalized reactions kinetics analysis and the criteria used to select the reactions that are important in the char zone.

ENERGY AND MOMENTUM TRANSFER IN THE CHAR ZONE

To compute the energy transferred and the pressure distribution in the char zone, it is necessary to solve the energy equation and momentum equation with appropriate boundary conditions. For steady flow of pyrolysis gases in a char zone of constant thickness, the energy equation has the following form [15]:

$$W_g \bar{C}_p \epsilon \frac{dT}{dz} - \frac{d}{dz}\left(k_e \frac{dT}{dz}\right) + \sum_{j=1}^{K+1} H_j R_j = 0 \quad (1)$$

convective heat transfer | conductive heat transfer | heat absorbed by chemical reactions

To describe the pressure distribution, a modified form of Darcy's equation was used which accounts for inertial effects that are important due to the high mass flux of degradation products. For the steady flow of an ideal gas in the char with varying mass flux, the following integral equation was obtained to predict the pressure distribution:

$$P = \left\{ P_L^2 + 2R \left[\epsilon/\gamma \int_z^L (W_g \mu \, T/\bar{M}) dz + \beta \int_z^L (W_g^2 \, T/\bar{M}) dz \right] \right\}^{1/2} \quad (2)$$

pressure loss due to viscous effects | pressure loss due to inertial effects

The energy absorbed in the char zone is equal to the difference between the heat flux at the high-temperature surface and the heat flux at the low-temperature surface. As shown later in Eq. (20), the energy absorbed for nonequilibrium flow in the char is given by:

$$q_{cz} = \epsilon \sum_{j=1}^{K} \int_{T_0}^{T_L} W_g x_j C_{P_j} dT + \sum_{j=1}^{K+1} \int_{T_0}^{T_L} H_j R_j / \left(\frac{d}{dz}\right) dT \quad (3)$$

heat absorbed due to change in gas enthalpy | heat absorbed by chemical reaction

Equations (1), (2), and (3) were solved numerically using programs written in FORTRAN IV on an IBM 7040 computer [15]. A subsequent section Generalized Reaction Kinetics Analysis, discusses the method used to compute the reaction rates of the simultaneous chemical reactions as they occur in the char zone.

However, before the calculations can be performed, two additional pieces of information must be known. These are the specific chemical reactions that occur in the char with their associated kinetic constants, and the initial composition of the pyrolysis gases entering the char zone. The 10 specific chemical reactions that are thought to occur in the char zone are listed in

Table 1. Important Chemical Reactions in the Char Zone in the Temperature Range of 500-2500°F

	Reaction	Activation energy kcal	Frequency factor, sec^{-1}
1.	$CH_4 = \frac{1}{2} C_2H_6 + \frac{1}{2} H_2$	78.0	7.60×10^{14}
2.	$C_2H_6 = C_2H_4 + H_2$	60.0	3.14×10^{13}
3.	$C_2H_4 = C_2H_2 + H_2$	23.0	2.57×10^{8}
4.	$C_2H_2 = 2C + H_2$	40.0	2.14×10^{10}
5.	$CH_4 = \frac{1}{2} C_2H_2 + \frac{3}{2} H_2$	86.5	$2.14 \times 10^{9} T^{-1}$
6.	$CH_4 = C + 2H_2$	16.2	$2.05\ T^{-1}$
7.	$C_6H_6 = 3C_2H_2$	52.0	1.4×10^{9}
8.	$C + H_2O = CO + H_2$	21.3	9.26×10^{3}
9.	$NH_3 = \frac{1}{2} N_2 + \frac{3}{2} H_2$	60.8	2.80×10^{6}
10.	$CH_4 + 2O_2 = CO_2 + 2H_2O$	20.6	1.5×10^{17}

Table 1, and the method of arriving at these reactions is discussed in the section entitled Criteria for Reaction Selection.

In Fig. 1 a comparison is shown of the temperature distribution for nonequilibrium, equilibrium, and frozen flow from the solution of the equations of change (continuity, momentum, and energy) for a surface temperature of 2500°F. As shown, the temperature distribution for nonequilibrium flow is only slightly less than that for frozen flow. This result is due to the chemical reaction rates in this temperature range, which produce a change in the pyrolysis gas composition. However, the temperature distribution for equilibrium flow is significantly different than that for nonequilibrium flow. This is a result of the energy absorbed due to the significant changes in pyrolysis gas composition, which is computed by considering the gases to be in thermodynamic equilibrium.

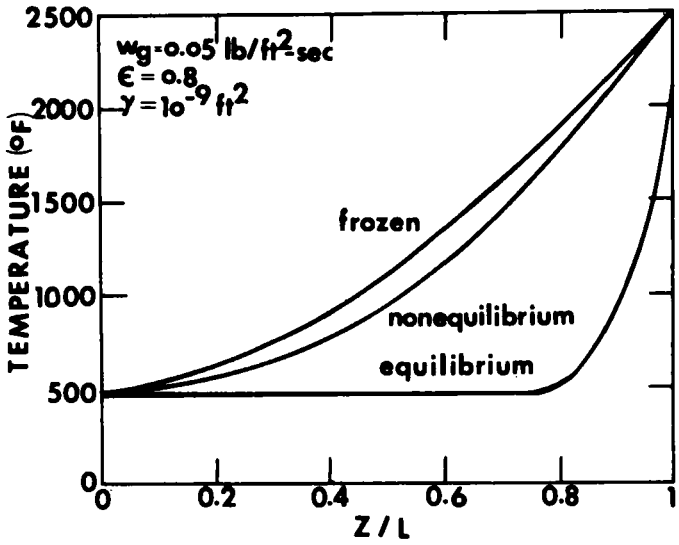

Fig. 1. Temperature profiles, T_L = 2500°F.

Although the temperature profile is essentially the same, there is a significant difference between the heat flux at the high-temperature surface for nonequilibrium and frozen flow, as seen in Table 2. This is mainly a result of the decomposition of methane to acetylene and hydrogen by reaction 5 in Table 1. This is seen in Table 2 by the change in degradation product composition from 500 to 2500°F. The energy absorbed, considering the flow in thermodynamic equilibrium, is much larger than that for nonequilibrium flow. Thus, if some means could be devised to increase the rate of reactions, there is the potential for a sizable reduction in heat shield weight.

Given in Table 2 are the pressure drops through the char calculated using Eq. (2) for nonequilibrium, equilibrium, and frozen flow. As would be expected, the pressure drop predicted by assuming the flow to be in equilibrium is less than that for either frozen or nonequilibrium flow since the viscosity is an increasing function of temperature. As would be expected, the pressure drops for nonequilibrium and frozen flow are essentially the same.

In Fig. 2 profiles similar to those in Fig. 1 are shown for a front-surface temperature of 2000°F. However, a comparison of the surface heat flux (Table 3) shows that there is a less significant difference between that for frozen flow and nonequilibrium flow. Consequently, the major energy absorption occurs in the temperature range of 2000-2500°F. This would

Table 2. Heat Flux, Pressure Drop, and Exit Gas Composition for Each Flow Type

Flow model	Heat flux at surface, Btu/ft^2-sec	Pressure drop, lb/ft^2	Midpoint temp., °F
Frozen	63.12	18.9	1045.7
Nonequilibrium	93.79	18.7	986.1
Equilibrium	271.25	9.8	540.9

Gas component	Mole % inlet gas composition	Mole % exit gas composition	
		Nonequilibrium	Equilibrium
Methane	55.47	3.4	0.10
Water	32.48	18.47	0.01
Nitrogen	8.06	4.61	4.21
Carbon dioxide	1.52	0.87	0.00
Hydrogen	1.45	58.27	77.03
Ammonia	0.02	0.01	0.00
Carbon monoxide	0.00	0.12	18.65
Ethane	0.00	0.16	0.00
Ethylene	0.00	0.52	0.00
Acetylene	0.00	13.73	0.00

be expected since the rate of reaction increases exponentially with temperature. Thus, it would also be expected that for cases with higher char temperatures the heat absorbed by chemical reactions would be much more significant. Work is currently in progress to extend these analyses to higher surface temperatures.

EXPERIMENTAL SIMULATION OF THE CHAR ZONE DURING ABLATION

Char Zone Thermal Environment Simulator

Experiments are being conducted to establish the accuracy of the nonequilibrium flow model with an experimental system that simulates the char zone during ablation. A schematic diagram of the char zone thermal environment simulator is shown in Fig. 3.

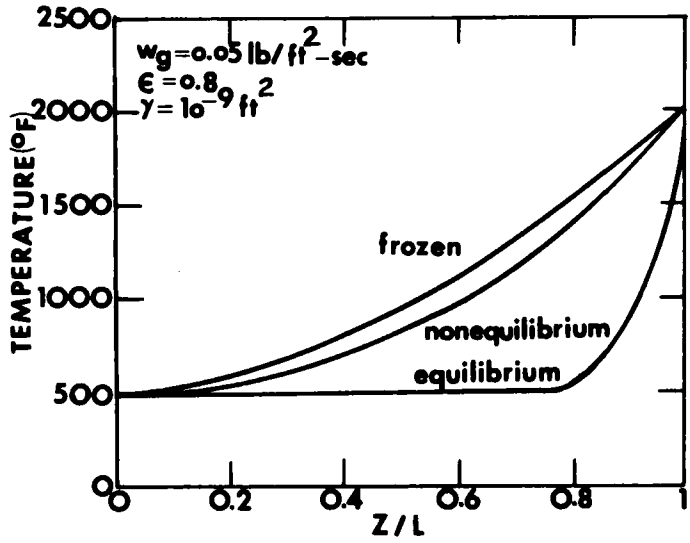

Fig. 2. Temperature profiles, T_L = 2000°F.

In this simulator actual chars formed in the arc jets at the Langley Research Center are utilized. Gas compositions typical of the degradation products are passed through the heated chars. Important variables are monitored with exit gas samples taken at specific time intervals.

Experimental Results

In Table 4 a comparison is made between typical experimental results and the models of nonequilibrium and equilibrium flow. The inlet composition is the concentration of the stream entering the char at T_0, and the outlet composition is the concentration leaving the front surface of the char at T_L. As shown, the amount of chemical reaction that actually takes place is only slight, and this is accurately predicted by nonequilibrium flow. The computed values of the composition agree within experimental error with the experimental values. For these temperature ranges the flow is essentially frozen (no chemical reaction).

If the pyrolysis gases were actually in thermodynamic equilibrium flowing through the char, there would have been a significant heat absorption due to reaction. In fact, nearly all of the methane would be decomposed and essentially all of the carbon dioxide would be converted. Thus, this model is an extremely poor characterization of the flow over this temperature range and results in unrealistically high surface heat flux values.

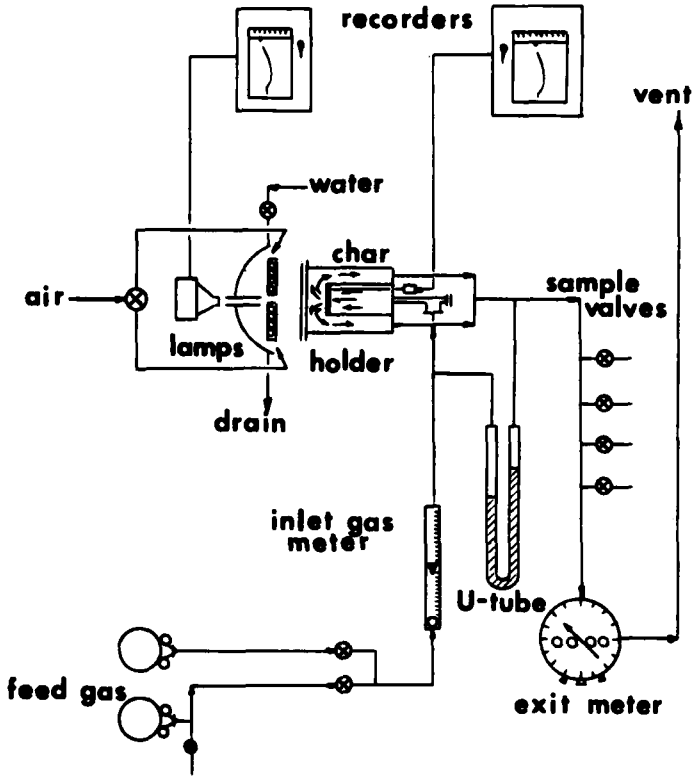

Fig. 3. Char zone thermal environment simulator.

The nonequilibrium flow temperature profile lies very near the profile for frozen flow, while the equilibrium flow deviates significantly, as would be expected. The energy absorbed due to chemical reactions is indicated by a slight increase in the surface heat flux over the frozen flow. However, the heat flux predicted for equilibrium flow is over six times that for nonequilibrium flow.

In conclusion, it can be stated that over the temperature range of the experiments only a small change in composition occurs due to chemical reactions as the gas flows through the char. The flow is essentially frozen. If the chemical species flowing through the char are assumed to be in thermodynamic equilibrium, there is a sixfold error in computing the surface heat flux, i.e., the energy absorbed in the char zone.

Table 3. Heat Flux, Pressure Drop, and Exit Gas Composition for Each Flow Type

Flow model	Heat flux at surface, Btu/ft²-sec	Pressure drop, lb/ft²	Midpoint temp., °F
Frozen	44.50	15.3	892.9
Nonequilibrium	46.07	15.1	864.6
Equilibrium	187.61	8.8	537.6

Gas component	Mole % inlet gas composition	Mole % exit gas composition	
		Nonequilibrium	Equilibrium
Methane	55.47	53.50	0.25
Water	32.48	31.83	0.05
Nitrogen	8.06	7.91	4.25
Carbon dioxide	1.52	1.50	0.01
Hydrogen	1.45	4.35	76.78
Ammonia	0.02	0.02	0.00
Carbon monoxide	0.00	0.08	18.65
Ethane	0.00	0.49	0.00
Ethylene	0.00	0.05	0.00
Acetylene	0.00	0.28	0.00

GENERALIZED REACTION KINETICS ANALYSIS

The purpose of this section is to present the equations that permit the calculation of the reaction rates for an arbitrary number of simultaneous chemical reactions involving an arbitrary number of chemical species. This is illustrated with the reactions given in Table 1. A chemical reaction can be written in general as:

$$\sum_{j=1}^{K} r_{ij} A_j \underset{k_{r_i}}{\overset{k_{f_i}}{\rightleftarrows}} \sum_{j=1}^{K} p_{ij} A_j \tag{4}$$

For this ith chemical reaction, the r_{ij} and p_{ij} represent the stoichiometric coefficients of the reactants and products, respectively, for species A_j. The forward and reverse reaction rate constants are k_{fi} and k_{ri}. There are a total of K chemical species.

Table 4. Comparison of Experimental and Calculated Results for the Various Flow Models[a]

Number	Mass flux, lb/ft²-sec	Temperatures, °F T_0	Temperatures, °F T_L	Gas component	Mole % inlet gas composition	Mole % exit gas composition EXP[b]	Mole % exit gas composition NEF	Mole % exit gas composition EF	Surface heat flux, Btu/ft²-sec FF	Surface heat flux, Btu/ft²-sec NEF	Surface heat flux, Btu/ft²-sec EF
V-11	0.00144	727.5	1575	Hydrogen	37.2	37.7	37.6	72.3	0.67	0.68	5.77
				Methane	32.5	29.5	31.9	1.0			
				Ethane	0.0	0.1	0.1	0.0			
				Ethylene	0.0	0.0	0.0	0.0			
				Acetylene	0.0	0.6	0.3	0.0			
				Nitrogen	15.5	15.5	15.4	11.3			
				Ammonia	0.0	0.0	0.0	0.0			
				Carbon dioxide Carbon monoxide	14.8	16.5	14.7	15.4			
				Water	0.0	0.0	0.0	0.0			

V-13	0.00635	770.0	1610	Hydrogen	37.2	38.2	37.3	73.0	2.94	2.95	25.3
				Methane	32.5	32.2	32.3	0.8			
				Ethane	0.0	0.1	0.1	0.0			
				Ethylene	0.0	0.0	0.0	0.0			
				Acetylene	0.0	0.2	0.2	0.0			
				Nitrogen	15.5	15.5	15.5	11.0			
				Ammonia	0.0	0.0	0.0	0.0			
				Carbon dioxide Carbon monoxide	14.8	13.9	14.8	15.2			
				Water	0.0	0.0	0.0	0.0			

[b]EXP = experimental, FF = frozen flow, NEF = nonequilibrium flow, EF = equilibrium flow.

[a]Char material data: low-density phenolic-nylon composite charred in Langley Research Center arc jets. Thickness = 0.25 in., CSA = 0.51–0.71 in.^{2}, porosity = 0.8, permeability = 1×10^{-9} ft^2.

For the rate of reaction of the jth species, R_j, this is given by the following equation for n chemical reactions:

$$R_j = \sum_{i=1}^{n} (p_{ij} - r_{ij}) \, k_{f_i} \prod_{j=1}^{K} c_j^{r_{ij}} - k_{r_i} \prod_{j=1}^{K} c_j^{p_{ij}} \tag{5}$$

where c_j is the concentration of component j in appropriate units.

This equation has the powers on the composition terms the same as the stoichiometric coefficients. However, it is not necessary to do this. If this is not the case for some of the reactions being used, it is only necessary to include two additional matrices besides r_{ij} and p_{ij} in the computer implementation.

To illustrate the use of Eqs. (4) and (5), the matrix form of the reactions listed in Table 1 are shown in Table 5. This is Eq. (4) for 10 reactions and 13 chemical species.

To illustrate the use of Eq. (5), the rate of reaction of methane (component 2) is given by the following:

$$R_2 = \sum_{i=1}^{10} (p_{i2} - r_{i2}) \left[k_{f_i} \prod_{j=1}^{13} c_j^{r_{ij}} - k_{r_i} \prod_{j=1}^{13} c_j^{p_{ij}} \right] \tag{6}$$

or expanding

$$\begin{aligned} R_2 = {} & (0-1) \left\{ k_{f_1} c_2 - k_{r1} c_1^{1/2} c_3^{1/2} \right\} + \\ & (0-1) \left\{ k_{f_5} c_2 - k_{r5} c_1^{3/2} c_5 \right\} + \\ & (0-1) \left\{ k_{f_6} c_2 - k_{r6} c_1^{2} c_6 \right\} + \\ & (0-1) \left\{ k_{f_{10}} c_2 \, c_{12}^{1/2} - k_{r10} c_8 c_{13} \right\} \end{aligned} \tag{7}$$

The above equation contains six other terms in the expanded form, but these are not included since the coefficients are zero. Of course this equation is not exactly correct since the powers on the compositions are different in some cases for the actual rate expressions. For example, the carbon-carbon dioxide reaction involves the surface area of carbon and not a "concentration" of carbon. To take the surface area of the char into account the reaction rate constant was modified, and the exponent of the carbon "concentration" was set equal to zero.

Table 5. Matrix Formulation of the Chemical Reactions Given in Table 1

$$\begin{bmatrix} 0\,1\,0\,0\,0\,0\,0\,0\,0\,0\,0\,0 \\ 0\,0\,1\,0\,0\,0\,0\,0\,0\,0\,0\,0 \\ 0\,0\,0\,1\,0\,0\,0\,0\,0\,0\,0\,0 \\ 0\,0\,0\,0\,1\,0\,0\,0\,0\,0\,0\,0 \\ 0\,1\,0\,0\,0\,0\,0\,0\,0\,0\,0\,0 \\ 0\,1\,0\,0\,0\,0\,0\,0\,0\,0\,0\,0 \\ 0\,0\,0\,0\,0\,0\,1\,0\,0\,0\,0\,0 \\ 0\,0\,0\,0\,0\,1\,0\,0\,0\,0\,0\,0 \\ 0\,0\,0\,0\,0\,0\,0\,0\,1\,0\,0\,0 \\ 0\,1\,0\,0\,0\,0\,0\,0\,0\,0\,\tfrac{3}{2}\,0 \end{bmatrix} \begin{bmatrix} H_2 \\ CH_4 \\ C_2H_6 \\ C_2H_4 \\ C_2H_2 \\ C \\ C_6H_6 \\ CO_2 \\ CO \\ NH_3 \\ N_2 \\ O_2 \\ H_2O \end{bmatrix} = \begin{bmatrix} \tfrac{1}{2}\,0\,\tfrac{1}{2}\,0\,0\,0\,0\,0\,0\,0\,0\,0 \\ 1\,0\,0\,1\,0\,0\,0\,0\,0\,0\,0\,0 \\ 1\,0\,0\,0\,1\,0\,0\,0\,0\,0\,0\,0 \\ 1\,0\,0\,0\,0\,2\,0\,0\,0\,0\,0\,0 \\ \tfrac{3}{2}\,0\,0\,0\,\tfrac{1}{2}\,0\,0\,0\,0\,0\,0\,0 \\ 2\,0\,0\,0\,0\,1\,0\,0\,0\,0\,0\,0 \\ 0\,0\,0\,0\,3\,0\,0\,0\,0\,0\,0\,0 \\ 0\,0\,0\,0\,0\,0\,0\,2\,0\,0\,0\,0 \\ \tfrac{3}{2}\,0\,0\,0\,0\,0\,0\,0\,0\,\tfrac{1}{2}\,0\,0 \\ 0\,0\,0\,0\,0\,0\,0\,1\,0\,0\,0\,1 \end{bmatrix} \begin{bmatrix} H_2 \\ CH_4 \\ C_2H_6 \\ C_2H_4 \\ C_2H_2 \\ C \\ C_6H_6 \\ CO_2 \\ CO \\ NH_3 \\ N_2 \\ O_2 \\ H_2O \end{bmatrix}$$

CRITERIA FOR REACTION SELECTION

In a previous report [3] the literature was surveyed for the kinetics of the chemical reactions that could possibly occur in the char zone during ablation. At that time a number of reactions and species were located, and since then additional information has become available. However, it can be shown that not all of these possible reactions are important in the temperature range of interest. To determine the chemical reactions that would occur with a

Table 6. Composition of the Pyrolysis Gases from Phenolic Resin, Nylon, and a 50% Phenolic Resin-50% wt. Nylon Mixture in mole %

	Equilibrium composition calculated for the phenolic-nylon mixture [4]		Thermogravimetric and pyrolysis gas chromatographic analyses		
			Phenolic resin only [5]		Nylon-6 only [6][a]
Component	500°K	800°K	500°C	100–1000°C	400°C
H_2	1.45	43.25	15.1	50.1	0
H_2O	32.47	19.01	34.8	23.4	35.4
N_2	8.06	6.28	0	0	0
NH_3	0.02	0.02	0	0	0
HCN	10^{-11}	10^{-5}	0	0	0
CO	10^{-3}	1.85	4.5	5.5	0
CO_2	1.52	3.42	0.9	1.6	55.8
CH_4	56.48	26.15	7.8	10.0	0
C_2H_2	10^{-20}	10^{-10}	0	0	0
C_2H_4	10^{-20}	10^{-5}	0	0	0.4
C_6H_6	10^{-20}	10^{-13}	0.2	0.2	5.8
C_7H_8	b	b	0.8	0.3	0
C_6H_5OH	b	b	28.1	7.1	0
$(CH_3)_2C_6H_3OH$	b	b	7.8	1.8	0
Others	0	0	0	0	2.6
Total	100.00	100.00	100.00	100.00	100.00

[a]Liquid products obtained during pyrolysis were not identified (about 95% of the total pyrolysis products).

[b]Not considered, due to the lack of necessary free energy data.

significant conversion in the char, two procedures were used. One procedure consisted of computing the conversion of one reaction of an equal molal mixture of reactants flowing isothermally through the char [15]. The other procedure consisted of estimating the species and the composition that entered the char zone from thermogravimetric analysis, pyrolysis gas chromatographic analysis, and thermodynamic equilibrium calculations. A comparison of the initial composition from this latter approach is given in Table 6. These two procedures combined determine the important reactions that occur in the char.

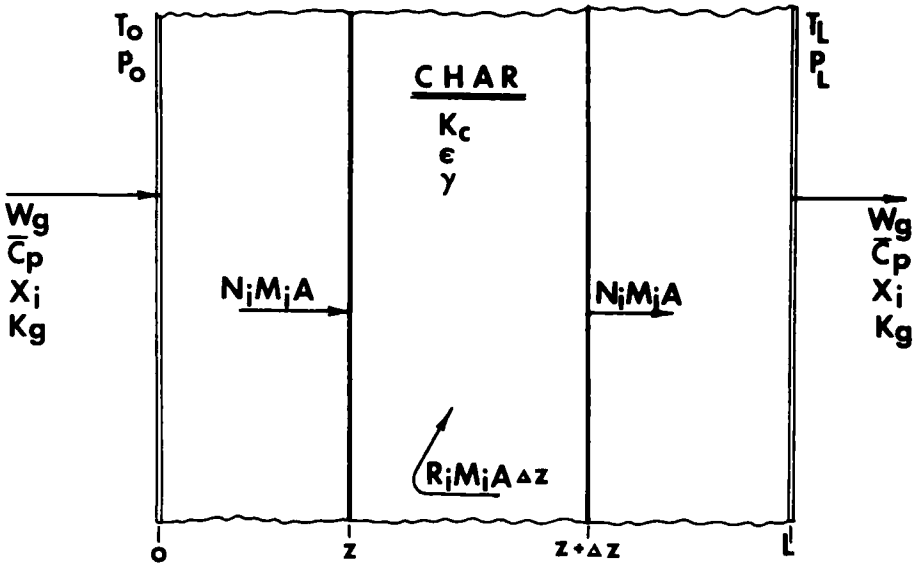

Fig. 4. Diagram of the char zone.

DEVELOPMENT OF EQUATIONS OF CHANGE FOR FLOW IN THE CHAR ZONE

Energy Equation

Referring to Fig. 4, the energy equation for one-dimensional flow of gases through a porous medium accompanied by chemical reactions is obtained by simplifying the general energy equation [7], and this gives:

$$W_g \cdot \epsilon \cdot \bar{C}p \cdot \left(\frac{dT}{dz}\right) = \epsilon \cdot \frac{d}{dz}\left[k_g \cdot \frac{dT}{dz}\right] - \epsilon \sum_{i=1}^{K} H_j R_j \tag{8}$$

The energy equation for the solid phase is:

$$0 = (1-\epsilon) \cdot \frac{d}{dz}\left[k_c \cdot \frac{dT}{dz}\right] - (1-\epsilon) \cdot H_c R_c \tag{9}$$

Adding Eqs. (8) and (9) and defining:

$$k_e = \epsilon \cdot \bar{k}_g + (1-\epsilon)\, k_c \tag{10}$$

as the effective thermal conductivity of the char, gives the differential equation that describes the energy transfer in the char zone:

$$W_g \cdot \epsilon \cdot \bar{C}_p \cdot \left(\frac{dT}{dz}\right) = \frac{d}{dz}\left[k_e \cdot \frac{dT}{dz}\right] \sum_{j=1}^{K+1} H_j R_j \tag{11}$$

For frozen flow in the char zone the above equation reduces to Eq. (12):

$$W_g \cdot \bar{C}_p \cdot \epsilon \cdot \left(\frac{dT}{dz}\right) = \frac{d}{dz}\left[k_e \cdot \left(\frac{dT}{dz}\right)\right] \tag{12}$$

Expanding and rearranging results in a second-order, ordinary differential equation which when solved gives the temperature profile in the char.

$$\frac{d^2T}{dz^2} = \frac{dT}{dz}\left[\frac{W_g \bar{C}_p \epsilon}{k_c} - \left(\frac{dk_e}{dT}\right)\left(\frac{dT}{dz}\right)\left(\frac{1}{k_c}\right)\right] \tag{13}$$

The energy equation for flow with chemical reaction is:

$$\frac{d^2T}{dz^2} = \frac{dT}{dz}\left[\frac{W_g \bar{C}_p \epsilon}{k_c} - \left(\frac{dk_e}{dT}\right)\left(\frac{dT}{dz}\right)\left(\frac{1}{k_c}\right) + \frac{1}{\left(\frac{dT}{dz}\right)} \sum_{j=1}^{K+1} H_j R_j\right] \tag{14}$$

In Eqs. (13) and (14), the surface temperatures are specified defining a two-point boundary value problem. Therefore, an iterative procedure to find the correct initial slope that satisfies the boundary conditions was required to define the temperature profile in the char.

Momentum Equation

To obtain the pressure distribution within the char zone, the momentum equation for flow in a porous medium must be solved. Because of the relatively high gas mass flux values ($W_g \cong 0.06$ lb/ft^2-sec), inertial as well as viscous effects must be included. The equation with these terms is given below for one-dimensional flow in a porous medium:

$$-\frac{dP}{dz} = \epsilon\mu u/\gamma + \beta\rho u^2 \tag{15}$$

where $\epsilon\mu u/\gamma$ represents the viscous term and $\beta\rho u^2$ the inertial term [11].

To obtain an equation applicable across a finite char thickness, the continuity equation, $W_g = \rho u$, and the ideal gas law, $\rho = P\bar{M}/RT$, are combined with Eq. (15) to give:

$$-PdP = \frac{RT}{\bar{M}} \quad (\epsilon\mu W_g/\gamma + \beta W_g^2)dz \tag{16}$$

Integrating this equation from the front surface where the pressure is P_L to any point P into the char at z gives:

$$P = \left\{P_L^2 + 2R\left[\frac{\epsilon}{\gamma}\int_{z=z}^{z=L}\frac{W_g\mu T dz}{\bar{M}} + \beta\int_{z=z}^{z=L}\frac{W_g^2 T dz}{\bar{M}}\right]\right\}^{1/2} \tag{17}$$

Typical values for γ and β used in the computation were 1×10^{-9} ft^2 and 5×10^4 ft^{-1}, respectively.

Heat Flux at the Char Surfaces

The heat fluxes at the char surfaces and the heat transfer by conduction to and from the surface are given by:

$$q_L = k_e \left.\frac{dT}{dz}\right|_{z=L} \quad \text{and} \quad q_o = k_e \left.\frac{dT}{dz}\right|_{z=0} \tag{18}$$

Frozen Flow. Integrating Eq. (12) for frozen flow gives:

$$q_{cz} = q_L - q_o = k_e \left.\frac{dT}{dz}\right|_{z=L} - k_e \left.\frac{dT}{dz}\right|_{z=0}$$

$$= \int_{T_o}^{T_L} W_g \bar{C}_p dT \tag{19}$$

where q_{cz} is the heat absorbed by a reaction gas mixture of K components.

Flow with Chemical Reaction. Integrating Eq. (11) for flow with chemical reaction gives:

$$q_{cz} = \epsilon \sum_{i=1}^{K} \int_{T_o}^{T_L} W_g(C_{p_j})\, x_j\, dT + \sum_{i=1}^{K+1} \int_{T_o}^{T_L} [(H_i R_i)/(dT/dz)]\, dT \tag{20}$$

where q_{cz} is the heat absorbed by a reacting gas mixture of K components.

Physical Properties

In order to solve Eq. (1) and (2) the values of the physical properties as functions of temperature are needed. For the heat capacity of each component the usual polynomial form is employed as shown below, where the values of the coefficients are obtained from Hougen et al. [8] and McBride et al. [9].

$$C_{pi} = a + bT + cT^2 + dT^3 + eT^4 \tag{21}$$

The mean heat capacity of the gas mixture is calculated using a molal weighted average as shown below:

$$\bar{C}_p = \sum_{i=1}^{K} C_{pi} \cdot y_i \tag{22}$$

The overall thermal conductivity as a function of the gas conductivity, the char conductivity, and the porosity is given by Eq. (10).

$$k_e = \epsilon \cdot \bar{k}_g + (1 - \epsilon) \cdot k_c \tag{23}$$

In this study, experimental data reported for the char conductivity were taken to be equal to the overall thermal conductivity. The reason is that the thermal conductivity measurements were made for char materials containing an inert gas in the pores. The equation for the char conductivity was obtained by a least-square fit of the data reported for an inert gas within the pores of the char [10].

NOMENCLATURE

A	cross-sectional area of the char zone
c	concentration
H_j	enthalpy per unit mass of component j
K	number of gaseous species
k_f	forward reaction rate constant
k_r	reverse reaction rate constant
L	width of char zone
$\bar{M}$	average molecular weight of the pyrolysis gases
M_j	molecular weight of component j
N_j	molal flux of component j

n number of chemical reactions
p_{ij} stoichiometric coefficients of the products
Q volumetric flow rate
q heat flux
R universal gas constant
R_j reaction rate of component j in moles per unit time per unit volume
r_{ij} stoichiometric coefficients of the reactants
S_t average residence time
u velocity of the pyrolysis gases in the pores of the char
V volume of the char
W_g mass flux of gas in the char pores
X_j conversion of component j
x_j mole fraction of component j
z coordinate axis in the direction of the pyrolysis gas flow in the char
β inertial coefficient of Eq. (15)
γ permeability
Δ forward difference operator
ϵ porosity
ρ density
μ viscosity

Subscripts

cz refers to char zone
i refers to chemical reactions
j refers to species
o refers to initial value
L refers to final value

ACKNOWLEDGMENT

This research was sponsored by the National Aeronautics and Space Administration under Grant NGR 19-001-016, and their support is gratefully acknowledged.

REFERENCES

[1] G. C. April, E. G. del Valle, and R. W. Pike, NASA-CR-77026, Reacting Fluids Laboratory, Louisiana State University, July 1, 1966.

[2] G. C. April, E. G. del Valle, and R. W. Pike, *Paper No. 13d*, National Meeting of the AIChE, Salt Lake City, Utah, May 21-24, 1967.
[3] R. W. Pike, *Langley Working Paper 181*, NASA, January 21, 1966.
[4] E. G. del Valle, G. C. April, and R. W. Pike, *Paper No. 13e*, National Meeting of the AIChE, Salt Lake City, Utah, May 21-24, 1967.
[5] G. F. Sykes and J. B. Nelson, *Preprint 7B*, 61st AIChE National Meeting, Houston, Texas, February 19-23, 1967.
[6] S. L. Madorski, *Thermal Degradation of Organic Polymers*, Wiley Interscience, New York, 1964.
[7] R. B. Bird, W. E. Stewart, and E. N. Lightfoot, *Transport Phenomena*, Wiley, New York, 1962, p. 562.
[8] O. A. Hougen, K. M. Watson, and R. A. Ragatz, *Chemical Process Principles, Part II*, Wiley, New York, 1962.
[9] B. J. McBride, S. Heimel, J. G. Ehbens, and S. Gordon, NASA SP-3001, 1963.
[10] R. G. Wilson, TND-2991, NASA, October 1965.
[11] P. C. Carman, *Flow of Gases Through Porous Media*, Butterworths, London, 1965, chapter VII.
[12] W. T. Engelke and C. M. Pyron, Jr., 6th Monthly Progress Report 7666-1531-4-VI, Southern Research Institute, February 15, 1966.
[13] J. Happel and L. Kramer, *Ind. Eng. Chem.*, **59** (1), 39 (1967).
[14] M. J. Shah, *Ind. Eng. Chem.*, **59** (5), 70 (1967).
[15] R. W. Pike, G. C. April, and E. G. del Valle, NASA-CR-66455, Reacting Fluids Laboratory, Louisiana State University, July 15, 1967.

Accepted by editor December 24, 1968
Received for publication January 3, 1969